HHS Public Access

Author manuscript

Nature. Author manuscript; available in PMC 2012 May 10.

Published in final edited form as:

Nature. ; 479(7372): 223–227. doi:10.1038/nature10533.

Genome sequencing reveals insights into physiology and longevity of the naked mole rat

Eun Bae Kim[1,*], **Xiaodong Fang**[2,*], **Alexey A. Fushan**[1,*], **Zhiyong Huang**[2,*], **Alexei V. Lobanov**[3], **Lijuan Han**[2], **Stefano M. Marino**[3], **Xiaoqing Sun**[2], **Anton A. Turanov**[3], **Pengcheng Yang**[2], **Sun Hee Yim**[3], **Xiang Zhao**[2], **Marina V. Kasaikina**[3], **Nina Stoletzki**[3], **Chunfang Peng**[2], **Paz Polak**[3], **Zhiqiang Xiong**[2], **Adam Kiezun**[3], **Yabing Zhu**[2], **Yuanxin Chen**[2], **Gregory V. Kryukov**[3,4], **Qiang Zhang**[2], **Leonid Peshkin**[5], **Lan Yang**[2], **Roderick T. Bronson**[6], **Rochelle Buffenstein**[7], **Bo Wang**[2], **Changlei Han**[2], **Qiye Li**[2], **Li Chen**[2], **Wei Zhao**[2], **Shamil R. Sunyaev**[3,4], **Thomas J. Park**[8], **Guojie Zhang**[2,#], **Jun Wang**[2,9,10,#], and **Vadim N. Gladyshev**[1,3,4,#]

[1]Department of Bioinspired Science, Ewha Womans University, Seoul, 120-750, Korea

[2]BGI-Shenzhen, Shenzhen, 518083, China

[3]Division of Genetics, Department of Medicine, Brigham and Woman's Hospital, Harvard Medical School, Boston, MA, 02115, USA

[4]Broad Institute of Harvard and MIT, Cambridge, MA 02142, USA

[5]Department of Systems Biology, Harvard Medical School, Boston, MA 02115, USA

[6]Rodent Histopathology Laboratory, Harvard Medical School, Boston, MA 02115, USA

[7]Department of Physiology and The Sam and Ann Barshop Institute for Longevity and Aging Studies, University of Texas Health Science Center, San Antonio, TX 78245, USA

[8]Department of Biological Sciences, University of Illinois at Chicago, Chicago, IL 60607, USA

[9]Novo Nordisk Foundation Center for Basic Metabolic Research, University of Copenhagen, Copenhagen, Denmark

[#]Correspondence and request for materials should be addressed to Guojie Zhang (zhanggj@genomics.org.cn), Jun Wang (wangj@genomics.org.cn), or Vadim N. Gladyshev (vgladyshev@rics.bwh.harvard.edu) .

[*]equal contribution

Supplementary Information is linked to the online version of the paper at www.nature.com/nature.

Author Contributions V.N.G. conceived the study. T.J.P. carried out animal work. A.A.T, M.V.K. and S.H.Y. prepared samples. X.F., Z.H., L.H., X.S., P.Y., X.Z., C.P., Z.X., Y.Z., Y.C., Q.Z., L.Y., B.W., C.H., Q.L., L.C., W.Z., G.Z. and J.W. performed genome sequencing and assembly. X.F., G.Z., and J.W. supervised genome sequencing and assembly. E.B.K., X.F., A.A.F., Z.H., A.V.L., S.S.M., L.P., G.Z. and V.N.G. performed genome and transcriptome analyses. Z.H., N.S., P.P., A.K. and S.R.S carried out genetic analyses. G.V.K., R.T.B. and R.B. discussed the data. All authors contributed to data interpretation. V.N.G. wrote the paper with significant contributions from E.B.K, X.F. A.A.F., Z.H., S.R.S., and G.Z., and input from all authors.

Author Information The NMR whole genome shotgun project has been deposited at DDBJ/EMBL/GenBank under the accession AFSB00000000. The version described in this paper is the first version, AFSB01000000. The mitochondrial sequence has been deposited at GenBank under the accession number JN242813. All short read data have been deposited into the Short Read Archive (http://www.ncbi.nlm.nih.gov/sra) under the accession number SRA030468. Raw sequencing data of the transcriptome have been deposited in Gene Expression Omnibus with the accession number GSE30337.

[10]Department of Biology, University of Copenhagen, Copenhagen, Denmark

Abstract

The naked mole rat (NMR, *Heterocephalus glaber*) is a strictly subterranean, extraordinarily long-lived eusocial mammal[1]. Although the size of a mouse, its maximum lifespan exceeds 30 years and makes this animal the longest living rodent. NMRs show negligible senescence, no age-related increase in mortality, and high fecundity until death[2]. In addition to delayed aging, NMRs are resistant to both spontaneous cancer and experimentally induced tumorigenesis[3,4]. NMRs pose a challenge to the theories that link aging, cancer and redox homeostasis. Although characterized by significant oxidative stress[5], the NMR proteome does not show age-related susceptibility to oxidative damage nor increased ubiquitination[6]. NMRs naturally reside in large colonies with a single breeding female, the "queen," who suppresses the sexual maturity of her subordinates[11]. NMRs also live in full darkness, at low oxygen and high carbon dioxide concentrations[7], and are unable to sustain thermogenesis[8] nor feel certain types of pain[9,10]. Here we report sequencing and analysis of the NMR genome, which revealed unique genome features and molecular adaptations consistent with cancer resistance, poikilothermy, hairlessness, altered visual function, circadian rhythms and taste sensing, and insensitivity to low oxygen. This information provides insights into NMR's exceptional longevity and capabilities to live in hostile conditions, in the dark and at low oxygen. The extreme traits of NMR, together with the reported genome and transcriptome information, offer unprecedented opportunities for understanding aging and advancing many other areas of biological and biomedical research.

We applied a whole genome shotgun strategy to sequence the genome of an individual male NMR (Table 1 and Supplementary Tables 1-3). The sequencing depth of 98.6% of the genome assembly was higher than 20X (Supplementary Fig. 1-4). The mitochondrial genome was also assembled. Approximately 25% of the NMR genome was represented by transposon-derived repeats, which is lower than in other mammals (40% in human, 37% in mouse, and 35% in rat genomes) (Supplementary Tables 4 and 5, Supplementary Fig. 5-7). The predicted NMR gene set included 22,561 genes (Table 1 and Supplementary Table 6), which is comparable to other mammals (e.g., 22,389 in human, 23,317 in mouse, and 22,841 in rat). Among these, 21,394 (94.8%) genes were transcribed (based on the RNA-seq data for 7 organs). More than 98% of NMR genes could be functionally annotated through homology approaches (Supplementary Table 7), and the quality of predicted genes was comparable to that of well-annotated mammalian genomes (Supplementary Tables 6 and 8 and Supplementary Fig. 8).

Most of the NMR genome (93%) showed synteny to human, mouse, or rat genomes (Supplementary Table 9), and pairwise comparisons suggested a relatively low rate of NMR genome rearrangements after the split from the murid common ancestor. We defined common synteny blocks in human, mouse, rat and NMR genomes and identified segmental duplications and lineage-specific indels (Supplementary Tables 10 and 11 and Supplementary Fig. 9). By analyzing single-copy orthologous groups, we constructed a phylogenetic tree involving NMR and other mammals (Fig. 1). As expected, NMR placed within rodents and its ancestor split from the ancestor of rats and mice approximately 73 million years ago, whereas the ancestor of NMR, mouse and rat split from rabbit

approximately 86 million years ago. Thus, in spite of some exceptional traits of NMR, the overall properties of its genome appeared to be similar to those of other mammals.

Lineage-specific gene family expansions may be associated with the emergence of specific functions and physiology. Compared to other mammals, NMR showed a moderate number of gene families under expansion and contraction (Fig.1b), including 96 NMR lineage-specific gene families (Fig. 2). Analysis of syntenic regions identified 750 gained and 320 lost NMR genes (Supplementary Tables 12-14). At least 75.5% of gained genes showed evidence of transcription, and the lost genes were enriched for ribosome and nucleoside biosynthesis functions (Supplementary Table 15). We also identified 244 pseudogenes, containing 183 frameshift and 119 premature termination events (Supplementary Tables 16 and 17). Functional categories enriched for pseudogenes included olfactory receptor activity (GO:0004984, $P < 0.001$, Fisher's exact test, 36 genes), visual perception (GO:0007601, $P = 0.015$, *CRB1*, *CRYBB3*, *GNAT2*, *GRK7*, *GUCA1B*, and *PDE6H*), spermatogenesis (GO: 0007283, $P = 0.044$, *ADAM29*, *ADC*, *CCIN*, *CCT6B*, *DEDD*, *OAZ3*, and *SHBG*), and possibly RING domain (SM00184, $P = 0.142$, *CNOT4*, *KCNRG*, *RNF5*, *TRIM17*, *TRIML1*, and *ZSWIM2*). The enrichment in the visual perception category appears to underlie the evolution of poor vision in NMR, whereas many RING domain-containing proteins act as ubiquitin ligases[12]. The levels of ubiquitinated proteins in NMRs are lower than in mice and, unlike those in mice, do not change significantly with age[6].

Identification of genes that have undergone positive selection in the NMR lineage can provide useful pointers to the evolution of its unique traits. 45 genes (0.4%) were identified as positively selected in the NMR lineage at the false discovery rate (FDR) of 0.01 and 141 genes (1.2%) at the FDR of 0.05 (Supplementary Table 18). 12 out of the 45 genes (corresponding to the FDR of 0.01) passed a strict manual inspection for the alignment quality. In comparison, 0.7% of genes were predicted to be positively selected in the human lineage from high quality alignments and using ROM correction for multiple testing[13]. Interestingly, our set included *TEP1* encoding a telomerase component and *TERF1*, a telomeric repeat binding factor identified at the FDR of 0.05 (Supplementary Fig. 10). *TERF1* gene product is one of six proteins contributing to the shelterin complex that shapes and protects telomeres[15] and that has been proposed to regulate telomere length[16].

To gain further insights into biological processes that underlie the exceptional traits of NMR, we identified 39 NMR proteins containing 45 amino acid residues unique among orthologs present in 36 vertebrate genomes (Supplementary Table 19). This gene set included cyclin E1 (*CCNE1*), uncoupling protein 1 (*UCP1*) and γ-crystallin (*CRYGS*), which are associated with G1/S transition during the cell cycle, thermogenesis and visual function, respectively. Noteworthy are also *APEX1*, a multifunctional DNA repair enzyme, *RFC1*, replication factor C, and *TOP2A*, a DNA topoisomerase that controls the topologic states of DNA during transcription. This set also contained 8 genes designated as cancer-related genes[14]. Finally, *TOP2A*, along with *TEP1* and *TERF1* from the set of positively selected genes, are part of a 5-protein complex of alternate lengthening of telomere pathway[17]. Overall, these analyses point to altered telomerase function in NMR, which may be related to the evolution of the extended lifespan and cancer resistance.

We also identified 1.87 million heterozygous SNPs. This results in an estimated nucleotide diversity (mean per nucleotide heterozygosity) of 7×10^{-4}, which is much lower than in mouse and rat populations and is comparable to nucleotide diversity observed in humans. Transition nucleotide changes were observed twice more frequently than transversions indicating that variant calls reproduce expected properties of natural variation in other mammals. The low level of nucleotide diversity may reflect a low effective size of NMR population, but may also be due to a high level of inbreeding, a reduced mutation rate or high efficiency of the repair systems. The variation of diversity along the genome was consistent with inbreeding in the NMR population. In protein-coding regions of the genome, our analysis identified 10,951 non-synonymous and 8,616 synonymous SNPs. Their ratio is much higher than in other studied organisms, including human, which appears to signal relaxation of purifying selection in NMR, potentially as a consequence of reduced effective population size. Finally, we analyzed context dependency of NMR SNPs (Supplementary Fig. 11). Relative rates of nucleotide changes and nucleotide context dependencies were similar to those observed in human polymorphism with the exception of a relative reduction of SNPs due to CpG mutations. This was caused by a combination of a relatively low CpG density in the NMR genome and a higher fraction of CpG di-nucleotides within CpG islands compared to the human genome. CpG density was only 0.19 of the expected under GC content, which is lower than in human, dog and panda genomes, but is similar to the mouse genome. However, in comparison to mouse, a higher fraction of CpG di-nucleotides was concentrated in CpG islands. CpG di-nucleotides within CpG islands contribute less to genetic variation because of lower methylation rate and possibly also due to selection.

Long lifespan is a key feature of NMR. To study aging and longevity, we obtained RNA-seq data for brain, liver and kidney of newborn, young adult (4-year old) and old adult (20-year old) NMRs (Supplementary Table 20). In contrast to other mammals, few genes showed differential expression between 4 and 20 year old NMRs, especially in the brain (Supplementary Tables 21-23). A recent study identified 33 under-expressed and 21 over-expressed genes in the human brain during aging[18]. Of these, 32 genes did not show consistent expression changes with aging in NMR, 30 had stable expression and 2 changed in the opposite direction compared to human brain (Supplementary Table 21). For example, *CYP46A1* and *SMAD3* were down-regulated in the human brain, but showed elevated expression in the NMR brain. The product of *CYP46A1* gene is a mediator of cholesterol homeostasis that influences the tendency of Aβ to aggregate. The product of *SMAD3* is a modulator of TGF-β signaling, playing a role in cancer development by slowing down the rate of cell proliferation. Elevated expression of *SMAD3* in NMR during aging may help optimize the rate of cell death, protecting NMRs from cancer.

A previous meta-analysis of age-related gene expression in mice, rats and humans revealed 56 consistently overexpressed and 17 underexpressed genes[19]. However, many of these genes did not show the same expression changes, suggesting that different regulatory mechanisms may underlie NMR longevity (Supplementary Tables 22 and 23). For example, genes related to degradation of macromolecules, such as *GSTA1, DERL1,* and *GNS,* were not up-regulated with age in NMRs. We also found that genes encoding mitochondrial proteins (*NDUFB11*, *ATP5G3*, and *UQCRQ*) were not down-regulated, consistent with

stable maintenance of mitochondrial function during aging. It is also of interest that *TERT* (telomerase reverse transcriptase) showed stable expression regardless of age (Supplementary Fig. 12). This finding is consistent with the role of the telomerase complex highlighted by positive selection on *TEP1* and *TERF1*. Overall, transcriptome and sequence data revealed different (compared to humans, mice and rats) patterns of NMR genes, which may underlie longevity mechanisms in this animal.

Non-shivering thermogenesis is a major heat production process in mammals that mainly depends on the action of *UCP1*, one of the 39 vertebrate genes that changed uniquely in NMR (Supplementary Table 19). UCP1 featured changes in amino acids Gln146, Arg263, Trp264 and Thr303, with the latter two residues being subject to positive selection ($P < 0.05$, likelihood ratio test for the branch-site model, $n = 30$) and Arg263 and Trp264 located in the conserved nucleotide binding motif (Fig. 3a). With Arg-Trp in place of the rigid Gly-Pro in the key regulatory site, UCP1 is expected to lose the tight regulation by purine nucleotides as inhibitors and fatty acids as activators (Fig. 3b and 3c). The same loop also features two positively charged Lys residues followed by a negatively charged residue (also a unique combination), that should markedly affect the local electrostatic potential of UCP1. In addition, Gln146 replaced a conserved His involved in proton transport, and the same mutation was shown to decrease proton conductance of UCP1 five-fold[20]. Thr303 is located in the C-terminal motif (RqTxDCxT) required for binding purine nucleotides[21]. Taken together, these observations indicate a tight association of UCP1 function with the unique thermoregulation in NMR[22].

In mammals, switches between light and dark periods affect synthesis of a hormone melatonin, which modulates sleep and circadian rhythms. NMRs live in the natural dark habitat and their pineal glands, where melatonin is synthesized, are characterized by atrophy[23], but we found that the genes involved in melatonin synthesis (*TPH1*, *TPH2*, *DDC*, *AANAT* and *ASMT*) are intact. Interestingly, the expression of genes involved in the final two steps of melatonin synthesis was very low (*AANAT*) or undetectable (*ASMT*) in the NMR brain regardless of age (Supplementary Table 24 and Supplementary Fig. 13). Moreover, two major mammalian melatonin receptors (*MTNR1A* and *MTNR1B* encoding MT_1 and MT_2, respectively) were inactivated by mutations that introduce premature stop signals (Supplementary Fig. 14). Synteny analyses showed that these pseudogenes corresponded to mouse *MTNR1A* and *MTNR1B*. Although melatonin signaling appears to be disrupted in NMR, its circadian rhythms were maintained in terms of locomotor activity and body temperature when exposed to periodic light/dark changes[24]. Our finding is consistent with the previous report that MT_1/MT_2 knockout mice maintained essentially normal circadian rhythms[25]. These mice also showed decreased insulin secretion[25]. Likewise, our transcriptome analysis of NMR revealed decreased expression of genes involved in insulin/IGF-1 signaling in the liver compared to mice (Supplementary Fig. 15).

To explain the extraordinary resistance of NMR to cancer[3], a two-tier protective mechanism involving contact inhibition mediated by $p16^{Ink4a}$ and $p27^{Kip1}$ was proposed[4]. The involvement of $p16^{Ink4a}$ is unusual, since humans and mice only show contact inhibition mediated by $p27^{Kip1}$. We analyzed the gene locus and the transcriptome reads corresponding to tumor suppressors $p16^{Ink4a}$ and $p19^{Arf}$. As in mice, the $p16^{Ink4a}$ transcript consists of

three exons (Supplementary Fig. 16). However, sequence similarity in the last exon is low, and two early stop codons in the second exon were predicted to result in a shorter 14 kDa protein (Supplementary Fig. 17). The four ankyrin repeats were, however, intact and Thr69, a residue important for CDK6 binding, was conserved, so the function of the protein may be partially preserved (Supplementary Fig. 18). The $p19^{Arf}$ transcript consists of two exons, but four stop codons in the second exon should lead to a shorter 10 kDa protein (Supplementary Fig. 19-21).

NMR is also unique in that its skin and cutaneous C-fibers lack the neuropeptide Substance P, making this animal insensitive to certain types of pain[9,10]. Our analysis revealed the presence of intact *TAC1* encoding Substance P. However, NMR had a deletion in the core promoter region highly conserved among mammals (Supplementary Fig. 22). Thus, this neurotransmitter appears to be functional but may be under unique regulation.

We further examined the molecular basis for poor visual function and small eyes in NMR. Among the four vertebrate opsin genes (*RHO*, *OPN1LW*, *OPN1MW*, and *OPN1SW*), two (*OPN1LW* and *OPN1MW*) were missing (Table 2); this distinguishes NMR from other rodents with dichromatic color vision, such as mice, rats, and guinea pigs. However, NMR has intact *RHO* (rhodopsin) and *OPN4* (melanopsin), supporting the presence of rod-dominated retinae and the capacity to distinguish light/dark cues. Among about 200 genes associated with visual perception (GO:0007601) in humans and mice, almost 10% were inactivated or missing in NMR (Table 2 and Supplementary Fig. 23). These mammalian genes participate in crystallin formation, phototransduction in the retina, retinal development, dark adaptation, night blindness and color vision. For at least 10 of these genes, we observed relaxation of the functional constrain on NMR sequences by estimating the ratio of non-synonymous to synonymous substitutions, which corroborated the dysfunction of these genes. Inactivation of *CRYBA4*, one of microphthalmia-related genes, may be associated with the small-sized eyes, whereas inactivation of *CRYBA4* and *CRYBB3* and a NMR-specific mutation in *CRYGS* (Supplementary Table 19) with abnormal eye morphology[26]. Thus, while some genes responsible for vision are preserved in NMR, its poor visual function may be explained by deterioration of genes coding for various critical components of the visual system.

Further analysis revealed that substantial divergence of the NMR nuclear receptor corepressor Hairless from other mammalian orthologs and the presence of amino acid replacements associated with the hairless phenotype, which is consistent with the lack of fur in NMRs (Supplementary Fig. 24). In addition, we found substantial sequence variation in the sweet taste receptor and lack of many bitter taste receptors common to other mammals (Supplementary Fig. 25 and 26). In particular, NMR appears to lack the phenylthiocarbamide taste, a dominant genetic trait in humans, as well as several other common bitter tastes.

Air in NMR burrows is low in O_2 (~8%) and high in CO_2 (>20%) due to many animals sharing a limited air supply and poor gas exchange through soil[27]. To cope with the low O_2 conditions, NMR developed adaptive circulatory (altered hemoglobin oxygen affinity) and metabolic functions reducing metabolic rate and slowing down development[1,7,28,29]. To

obtain insights into this adaptation, we examined gene expression changes in several tissues of NMR subjected to 8% O_2 for one week (Supplementary Tables 25-31 and Supplementary Fig. 27-30). Many changes associated with energy metabolism and redox control were observed. Sequence analysis of NMR hypoxia-induced factor 1α (HIF1α) revealed a T407I exchange unique among mammals and located in the VHL-binding domain. In normoxia, VHL mediates ubiquitin-dependent degradation of HIF1α. In addition, NMR VHL harbors V166I exchange at a functionally important site. These amino acid changes are consistent with relaxation of ubiquitin-dependent degradation of HIF1α, and, thus, with adaptation to low oxygen conditions.

To summarize, sequencing and analysis of the NMR genome revealed numerous insights into the biology of this remarkable animal. In addition, this genome and the associated datasets offer the research communities working in aging, cancer, eusociality, and many other areas a rich resource that can be mined in numerous ways to uncover the molecular bases for the extraordinary traits of the one of the most unusual mammals, NMR. In turn, this information provides unprecedented opportunities for addressing some of the most challenging questions in biology and medicine, such as mechanisms of aging, the role of the genetic makeup in regulating lifespan, adaptations to extreme environments, hypoxia tolerance, thermogenesis, resistance to cancer, circadian rhythms, sexual development and hormonal regulation.

Methods Summary

The NMR genome was sequenced on the Illumina HiSeq 2000 platform. The sequenced individual NMR was from a captive breeding colony located at the University of Illinois, Chicago. The genome was assembled by using SOAPdenovo. We obtained 2.5 G contig sequences with N50 19.3 kbp and N90 4.7 kbp, and 2.7 G scaffold sequences with N50 1.6 Mbp and N90 0.3 Mbp. RNA-seq data (aging and low O_2 experiments) were for animals from the same colony. See Supplementary Information for data analysis and additional details.

Supplementary Material

Refer to Web version on PubMed Central for supplementary material.

Acknowledgements

We thank Pamela Colleen LaVinka for help in preparing NMR tissues and Nickilynn Estologa for help in preparing the manuscript. We acknowledge financial support from the WCU Program (R31-2008-000-10010-0), NIH (AG038004, AG021518 and CA080946), Shenzhen Municipal Government (ZYC200903240077A), National Natural Science Foundation of China (30725008), and National Science Foundation (0744979).

References

1. Edrey YH, Park TJ, Kang H, Biney A, Buffenstein R. Endocrine function and neurobiology of the longest-living rodent, the naked mole-rat. Exp. Gerontol. 2011; 46:116–123. [PubMed: 20888895]
2. Buffenstein R. Negligible senescence in the longest living rodent, the naked mole-rat: Insights from a successfully aging species. J. Comp. Physiol. B. 2008; 178:439–445. [PubMed: 18180931]

3. Liang S, Mele J, Wu Y, Buffenstein R, Hornsby PJ. Resistance to experimental tumorigenesis in cells of a long-lived mammal, the naked mole-rat (*Heterocephalus glaber*). Aging Cell. 2010; 9:626–635. [PubMed: 20550519]
4. Seluanov A, et al. Hypersensitivity to contact inhibition provides a clue to cancer resistance of naked mole-rat. Proc. Natl. Acad. Sci. USA. 2009; 106:19352–19357. [PubMed: 19858485]
5. Andziak B, et al. High oxidative damage levels in the longest-living rodent, the naked mole-rat. Aging Cell. 2006; 5:463–471. [PubMed: 17054663]
6. Pérez VI, et al. Protein stability and resistance to oxidative stress are determinants of longevity in the longest-living rodent, the naked mole-rat. Proc. Natl. Acad. Sci. USA. 2009; 106:3059–3064. [PubMed: 19223593]
7. Larson J, Park TJ. Extreme hypoxia tolerance of naked mole-rat brain. Neuroreport. 2009; 20:1634–1637. [PubMed: 19907351]
8. Buffenstein R, Woodley R, Thomadakis C, Daly TJ, Gray DA. Cold-induced changes in thyroid function in a poikilothermic mammal, the naked mole-rat. Am. J. Physiol. Regul. Integr. Comp. Physiol. 2001; 280:R149–55. [PubMed: 11124146]
9. Park TJ, et al. Selective Inflammatory Pain Insensitivity in the African Naked Mole-Rat (*Heterocephalus glaber*). PLoS Biology. 2008; 6:e13. [PubMed: 18232734]
10. Smith ES, Blass GR, Lewin GR, Park TJ. Absence of histamine-induced itch in the African naked mole-rat and “rescue” by Substance P. Mol. Pain. 2010; 6:29. [PubMed: 20497578]
11. Jarvis JUM. Eusociality in a mammal: cooperative breeding in naked mole-rat colonies. Science. 1981; 212:571–573. [PubMed: 7209555]
12. Deshaies RJ, Joazeiro CAP. RING domain E3 ubiquitin ligases. Annu. Rev. Biochem. 2009; 78:399–434. [PubMed: 19489725]
13. Schneider A, Souvorov A, Sabath N, Landan G, Gonnet GH, Graur D. Estimates of positive Darwinian selection are inflated by errors in sequencing, annotation, and alignment. Genome Biol. Evol. 2009; 1:114–118. [PubMed: 20333182]
14. Higgins ME, et al. CancerGenes: a gene selection resource for cancer genome projects. Nucl. Acids Res. 2007; 35:D721–D726. [PubMed: 17088289]
15. de Lange T. Shelterin: the protein complex that shapes and safeguards human telomeres. Genes Dev. 2005; 19:2100–2110. [PubMed: 16166375]
16. Van Steensel B, Lange T. Control of telomere length by the human telomeric protein TRF1. Nature. 2007; 385:740–741. [PubMed: 9034193]
17. Bhattacharyya S, et al. Telomerase-associated Protein 1, HSP90, and Topoisomerase IIA Associate Directly with the BLM Helicase in Immortalized Cells Using ALT and Modulate Its Helicase Activity Using Telomeric DNA Substrates. J. Biol. Chem. 2009; 284:14966–14977. [PubMed: 19329795]
18. Hong MG, Myers AJ, Magnusson PKE, Prince JA. Transcriptome-Wide Assessment of Human Brain and Lymphocyte Senescence. PLoS ONE. 2008; 3:e3024. [PubMed: 18714388]
19. de Magalhaes JP, Curado J, Church GM. Meta-analysis of age-related gene expression profiles identifies common signatures of aging. Bioinformatics. 2009; 25:875–881. [PubMed: 19189975]
20. Bienengraeber M, Echtay KS, Klingenberg M. H^+ transport by uncoupling protein (UCP-1) is dependent on a histidine pair, absent in UCP-2 and UCP-3. Biochemistry. 1998; 37:3–8. [PubMed: 9453747]
21. Porter RK. Uncoupling protein 1: A short-circuit in the Chemiosmotic process. J. Bioenerg. Biomembr. 2008; 40:457–461. [PubMed: 18958609]
22. Woodley R, Buffenstein R. Thermogenic changes with chronic cold exposure in the naked mole-rat (*Heterocephalus glaber*). Comp. Biochem. Physiol. A Mol. Integr. Physiol. 2002; 133:827–834. [PubMed: 12443938]
23. Quay WB. Pineal atrophy and other neuroendocrine and circumventricular features of the naked mole-rat, *Heterocephalus glaber* (Rüppell), a fossorial, equatorial rodent. J. Neural. Transm. 1981; 52:107–115. [PubMed: 7288432]
24. Riccio AP, Goldman BD. Circadian rhythms of locomotor activity in naked mole-rats (Heterocephalus glaber). Physiol. Behav. 2000; 71:1–13. [PubMed: 11134679]

25. Mühlbauer E, Gross E, Labucay K, Wolgast S, Peschke E. Loss of melatonin signalling and its impact on circadian rhythms in mouse organs regulating blood glucose. Eur. J. Pharmacol. 2009; 606:61–71. [PubMed: 19374844]

26. Nikitina NV, et al. Postnatal development of the eye in the naked mole rat (*Heterocephalus glaber*). Anat. Rec. A Discov. Mol. Cell. Evol. Biol. 2004; 277:317–337. [PubMed: 15052660]

27. Bennett, NC.; Faulkes, CG. African mole-rats: ecology and eusociality. Cambridge University Press; 2000.

28. McNab BK. The influence of body size on the energetics and distribution of fossorial and burrowing mammals. Ecology. 1979; 60:1010–1021.

29. Johansen K, Lykkeboe G, Weber RE, Maloiy GM. Blood respiratory properties in the naked mole rat *Heterocephalus glaber*, a mammal of low body temperature. Respir. Physiol. 1976; 28:303–314. [PubMed: 14363]

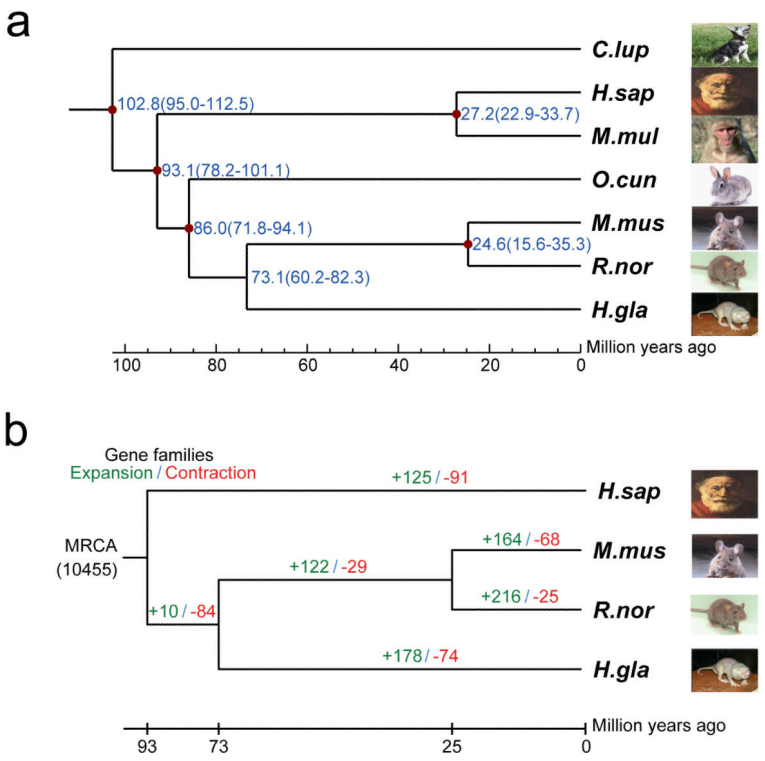

Figure 1. Relationship of NMR to other mammals

a, Estimation of the time of divergence of NMR and 6 other mammals based on orthology relationship. Distances are shown in millions of years. **b**, Expansion and contraction in gene families. Numbers designate genes gained and lost since the split from the common ancestor.

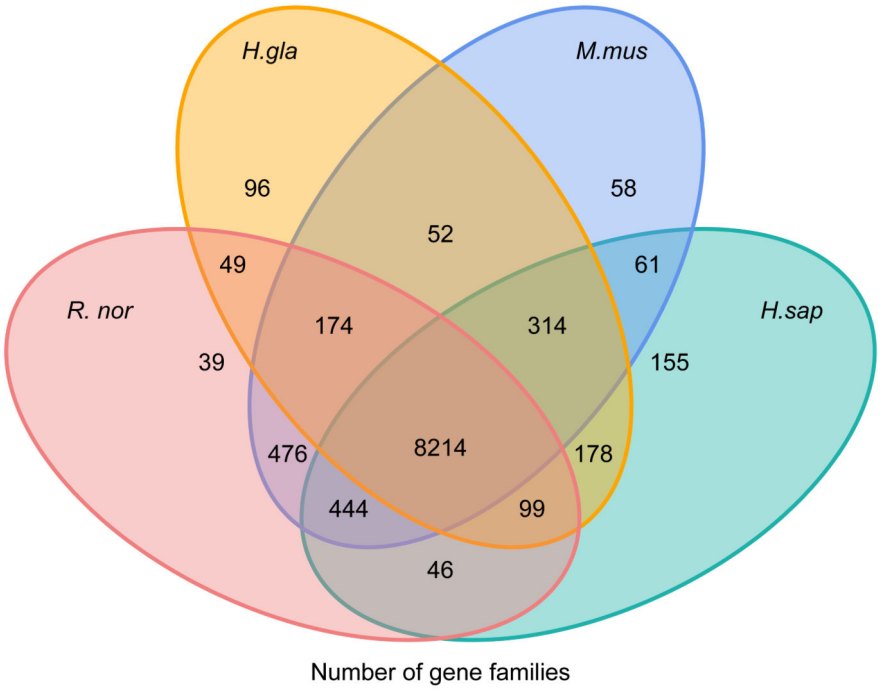

Figure 2. Common and unique NMR gene families

This Venn diagram shows unique and overlapping gene families in NMR (H. gla), rat (R. nor), mouse (M. mus) and human (H. sap).

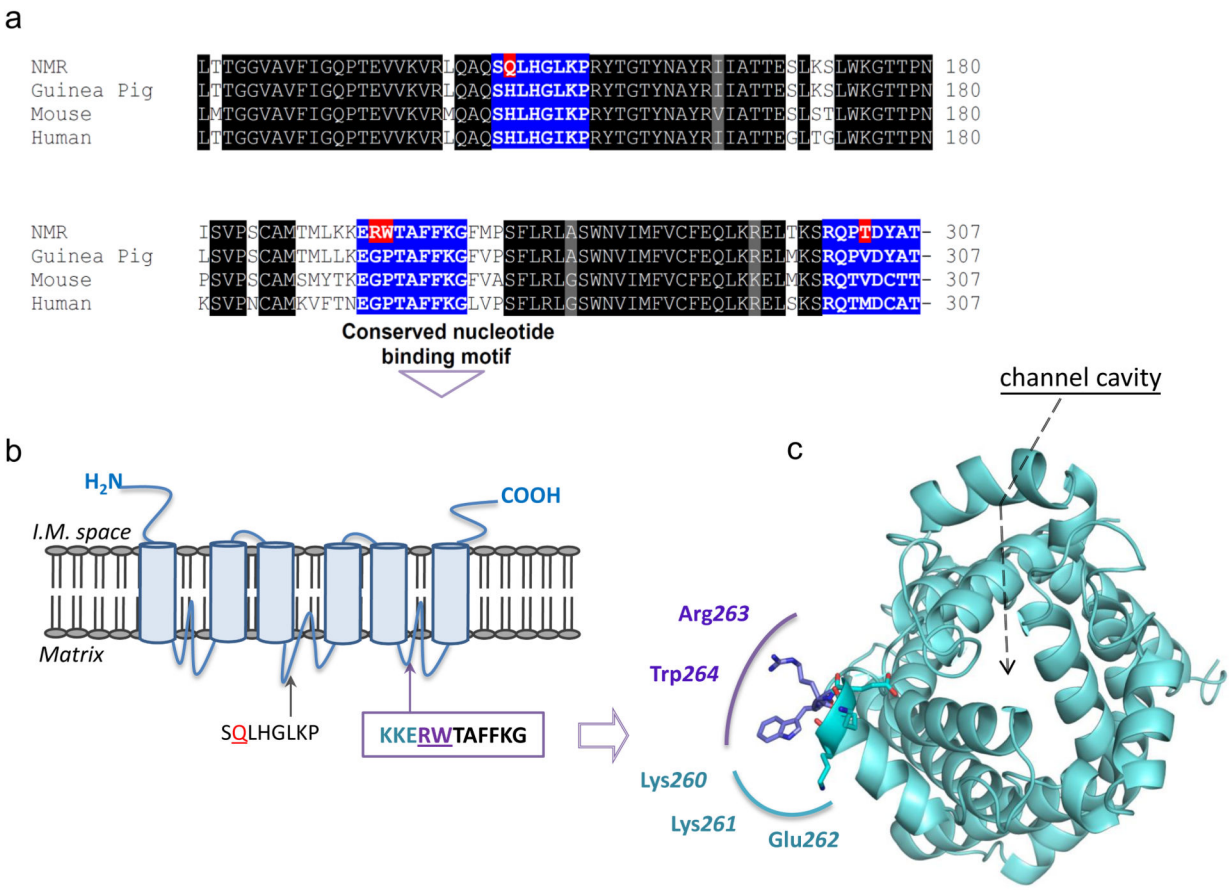

Figure 3. Unique changes in UCP1 and their roles in thermoregulation

a, Alignment of mammalian UCP1 sequences. Amino acids unique to NMR are highlighted in red, and conserved motifs in blue. **b**, Topology of UCP1. Regions affected in NMR are highlighted. **c**, Structural model of UCP1. Location of the channel and the nucleotide-binding loop with altered sequences in NMR are shown.

Table 1

Global statistics of the NMR genome.

(a) Sequencing			
	Insert size	**Total data (Gb)**	**Sequence coverage (X)**
	170~800 bp	126.52	47
Pair end libraries	2~20k	120.66	45
	Total	247.18	92
(b) Assembly			
	N50 (kb)	Longest (kb)	Size (Gb)
Contigs	19.3	179	2.45
Scaffolds	1,585	7,787	2.66
(c) Annotation			
	Number	Total length (Mb)	% of the genome
Repeats	3,090,116	666.7	25
Genes	22,561	722.3	27.1
CDS	181,641	32.5	1.2

Table 2

Visual perception genes that are inactivated or are missing in the NMR genome.

Gene	Inactivation event	Time of gene loss	ω0 (average)	ω1 (other)	ω2 (NMR)	P-value
RBP3	F	NMR	0.121	0.085	0.232	1.187E-11
ARR3	F/S	NMR	0.420	0.260	0.912	6.263E-06
PDE6C	F	NMR	0.171	0.139	0.316	0.0001
GUCA1B	F	NMR	0.083	0.056	0.217	0.001
GJA10	F/S	NMR	0.308	0.248	0.524	0.002
GUCY2E	F	NMR	0.124	0.105	0.182	0.002
CRYBA4	S	NMR	0.055	0.036	0.123	0.001
GNAT2	F	NMR	0.055	0.039	0.108	0.017
SLC24A1	F	NMR	0.389	0.355	0.517	0.035
CRYBB3	S	NMR	0.071	0.048	0.122	0.037
RP1L1	S	NMR	0.448	0.424	0.513	0.186
GRK7	F	NMR	0.154	0.135	0.201	0.335
PDE6H	F	NMR	0.091	0.082	0.127	0.648
EYS	F/S	Ancestor	-	-	-	-
GUCA1C	F	Ancestor	-	-	-	-
OPN1LW	L	NMR	-	-	-	-
OPN1MW	L	NMR	-	-	-	-
PRCD	L	NMR	-	-	-	-
RD3	L	NMR	-	-	-	-

F: frameshift, S: premature stop codon, L: complete loss detected with synteny information.

Ancestor/NMR indicates that the gene was lost in a rodent ancestor or NMR, respectively. The rate ratio (ω) of non-synonymous to synonymous substitutions was calculated by using human, mouse, rat and NMR sequences. ω0 is the average ratio in all branches, ω1 is the average ratio in non-NMR branches, and ω2 is the ratio in the NMR branch. A small *P*-value indicates that the two-ratio model fits the data better than the one-ratio model.